Numerical characterization of silicon DC electro-osmotic pumps: the role of the micro channel geometry

Michela GERI [1], Marco LORENZINI [1] , Gian Luca MORINI [1,*]

* Corresponding author: Tel.: +39 051203381; Fax: +39 051 2093296; Email: gianluca.morini3@unibo.it
1: DIENCA, Alma Mater Studiorum – Università di Bologna, IT

Abstract A numerical analysis of silicon DC open channel EOPs is presented to show which parameters should be taken into account in the design of these devices. Particular attention is paid to the influence of the channel cross-section geometry on pump behavior, especially in relation to the electrical properties of the fluid. Rectangular and trapezoidal, micro and nano channels chemically etched on silicon wafers are considered and a broad range of operative conditions are analyzed. In order to make all the results available, two user-friendly correlations that predict the characteristic curves of the pumps are given as functions of the relevant parameters. The EOP model used to obtain the results is explained extensively, as well as the method used to solve it. A brief discussion on the domain in which it applies is also presented.

Keywords: Electro-osmotic Pumps, Microflows, Silicon micro and nano channels

1. Introduction

Electro-osmotic pumps (EOPs) move fluids inside micro channels by means of an externally imposed electric field. The flow obtained by electro-osmosis is caused by the motion of a ionized liquid near to a stationary charged surface when an electric field is applied (Probstein, 1994). Most surfaces spontaneously acquire a finite charge density when in contact with an aqueous solution, inducing an uneven distribution of charges in the liquid bulk (Hunter, 1981). This happens in the fluid layer near the wall, called Electrical Double Layer (EDL), whose extension varies significantly with the channel dimensions and the electrolyte concentration.

EOPs have been developed in the last few decades along with the diffusion and advance of microfluidics in several fields (Manz *et al.*, 1990; Chen and Santiago, 2002; Laser and Santiago, 2004). More recently their use has been further spurred by the development of nanofluidics and biomedicine where mechanical pumps are at a disadvantage because of the presence of high pressure drops, the manufacturing of micro or even nano scale moving components and possible fluid contamination (Karniadakis *et al.*, 2005). Several configurations have been considered, namely DC and AC pumps, both of the *open channel* type, i.e. made of straight single or multiple parallel channels (Lazar and Karger, 2002), and of *packed column* as well as *porous monolith* and *porous membrane* type, in which a porous medium is used to extend the contact area between the fluid and the wall (Yao and Santiago, 2003; Yao *et al.*, 2003; Litster *et al.*, 2010, Wang *et al.*, 2009).

Most open channel EOPs fabricated on silicon substrates have channels whose cross-section is either rectangular or trapezoidal (Morini, 2004). In particular, channels obtained from chemical etching on wafers of <100> silicon have a trapezoidal cross-section, whose apex angle is θ=54.74°, while those produced with <110> silicon have a rectangular cross-section, with θ=90° (Fig. 1).

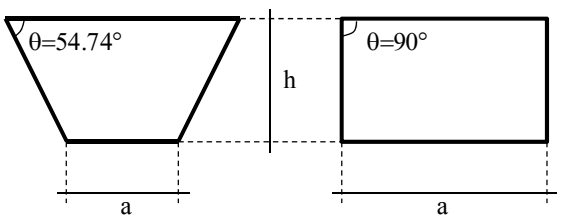

Fig. 1. Typical cross sections of silicon micro channels made by chemical etching.

A large part of the theoretical studies on EOPs published up to now have focused on channel shapes such as cylindrical and planar (Burgreen and Nakache, 1964; Rice and Whitehead, 1965; Hildreth, 1970; Masliyah and Bhattacharjee, 2006; Bruus, 2007), for which a significant simplification of the governing equations allows to find close analytical solutions. Sometimes these solutions have been employed to analyze complex geometries to predict the pump behavior (Chen and Santiago, 2002), especially for very narrow channels which are widely used at nano scales. When a simplified analytical solution is not available, numerical solutions can always be found to characterize these components and several numerical investigations have already been presented in the literature for specific configurations (Arulanandam and Li, 2000), although their results are not readily available for practical use. In any case, not many studies consider realistic geometries for the cross-section of the channels, like those shown in Fig. 1, and a systematic study of the impact of geometry on the pump behavior has not been carried out till now. From the above considerations it follows that it is still of great importance to perform a thorough analysis of the influence of the channel geometry on the pump behavior, especially in relation to the electrical properties of the fluid. The results can be used to determine some user-friendly correlations to design EOPs in a broad range of operative conditions. The aim of this work is therefore to provide an insight into the operational behavior of EOPs, focusing on the generalized scaling analysis in the case of channels with a finite cross-section, both for a very thin and a finite EDL. Also, a practical purpose of the present study is the determination of easy to use correlations to predict the pump performance for all the operative conditions here considered.

2. Modeling

In this section, the mathematical model of an EOP and the numerical scheme used to solve it are discussed. In addition, some remarks on the limits of validity of this theoretical framework are presented in order to justify the numerical results.

2.1 Governing equations

A DC open channel EOP can be modeled considering an induced electro-osmotic flow inside a channel, acting against a constant back pressure. For an incompressible fluid with constant properties and a fully developed flow, the momentum equation can be written as:

$$\mu\nabla^2 u(\xi,\eta) = -\rho_e^{eq}(\xi,\eta)E_{ext} + \frac{dp}{d\omega} \qquad (1)$$

where $u(\xi,\eta)$ is the only non-zero component of the velocity field, that is, the component along the channel axis ω, and μ is the dynamic viscosity of the fluid. On the RHS, the first term is the electric force acting on diffusive ions at the solid/liquid interface, where ρ_e^{eq} is the net charge distribution over the channel cross-section, which is assumed not to be affected by the local velocity field, while E_{ext} is the applied electric field, supposed to be uniform; the last term is the pressure gradient along the channel. No-slip boundary conditions are applied at the wall. Since the electric force is assumed not to be influenced by the velocity field, neither in the charge distribution nor in the electric field, the equation is linear and can be solved with the superposition principle once the charge distribution is known. Assuming that ions are displaced as for the static case, when the liquid does not flow, and that no overlap of the EDLs occurs, the charge distribution can be determined by means of the Poisson equation of electrostatics (Burgreen and Nakache, 1964):

$$\varepsilon\nabla^2\phi(\xi,\eta) = -\rho_e^{eq}(\xi,\eta) \qquad (2)$$

where a flat-wall Boltzmann distribution of ions can be considered:

$$\rho_e^{eq}(\xi,\eta) = e\sum_{i=1}^{N} z_i n_{i\infty} \exp\left(-\frac{ez_i\phi(\xi,\eta)}{kT}\right) \qquad (3)$$

In Eq. (2) and (3), $\phi(\xi,\eta)$ is the unknown electric potential, ε is the permittivity of the liquid electrolyte, e is the magnitude of the elementary charge, z_i is the i^{th}-ionic species valence with the appropriate sign, $n_{i\infty}$ is the ionic number concentration at the neutral state

(ϕ=0), k is the Boltzmann constant and T is the thermodynamic temperature. The summation comprises all the N ionic species. Boundary conditions for Eq. (2) assume that the electric potential equals the so called *zeta-potential* (ζ) at the wall. Substituting Eq. (3) into Eqs. (1) and (2) yields a set of two uncoupled PDEs that are the governing equations for an open channel EOP. The energy equation is not needed because the model refers to isothermal flows. While the momentum equation is linear, the Poisson–Boltzmann equation is strongly non-linear, but a linearization can be performed if the Debye-Hückel approximation holds, i.e. if ions mainly act under the influence of their thermal energy (Rice and Whitehead, 1965).

In order to obtain a general solution of the model, it is convenient to have all the variables and the equations in a non-dimensional form. A proper non-dimensional reference system can be obtained dividing each coordinate of the dimensional frame by the hydraulic diameter D_h:

$$x := \frac{\xi}{D_h} \qquad y := \frac{\eta}{D_h} \qquad z := \frac{\omega}{D_h} \tag{4}$$

while, for the electric potential and the zeta-potential suitable non-dimensional expressions are:

$$\Phi := \frac{e\phi}{kT} \qquad \mathrm{Z} := \frac{e\zeta}{kT} \tag{5}$$

For the local velocity field, it is more expedient to use the following quantity:

$$U := \frac{u}{u_{EO}} = \frac{u}{\dfrac{\varepsilon\, \zeta\, E_{ext}}{\mu}} \tag{6}$$

where u_{EO} is the Helmholtz – Smoluchowski velocity (Probstein, 1994). Invoking the Debye-Hückel approximation and substituting all the non-dimensional quantities into Eqs. (1) and (2), it is easy to get the non-dimensional form of the governing equations, that is:

$$\begin{cases} \nabla^2\Phi(x,y) = (\kappa D_h)^2\,\Phi(x,y) \\ \nabla^2 U(x,y) = \dfrac{(\kappa D_h)^2}{\mathrm{Z}}\, G_{EO} - \dfrac{1}{\mathrm{Z}}\nabla^2\Phi(x,y) \end{cases} \tag{7}$$

where κ is the Debye-Hückel parameter:

$$\kappa := \left(\frac{e^2}{\varepsilon kT} \sum_{i=1}^{N} z_i^2 n_{i\infty} \right)^{1/2} \tag{8}$$

while the product κD_h defines a quantity known as the *electrokinetic diameter* (D_e), which accounts for both the electrical properties of the fluid and the geometrical characteristics of the channel, showing that their influence on the electro-osmotic flow is strictly correlated. In Eq. (7) an operational, non-dimensional number has been introduced, G_{EO}, whose definition is:

$$G_{EO} := -\frac{dP/d\omega}{eE_{ext}\sum_{i=1}^{N} z_i^2 n_{i\infty}} \tag{9}$$

where P is the difference between the fluid pressure p and a reference pressure p_0. This new non-dimensional group is the ratio between the pressure body forces and the electrical body forces acting on the fluid. It is therefore related to the electrical work that the pump can transfer to the fluid to move it against a fixed pressure gradient. At the same time, it can be seen as the pressure head that the pump can handle for a given electrolyte composition and a fixed electric field. The set of two linear uncoupled PDEs (7), with the following non-dimensional boundary conditions:

$$\begin{cases} \Phi\big|_{wall} = \mathrm{Z} \\ U\big|_{wall} = 0 \end{cases} \tag{10}$$

can be easily managed to obtain a semi-analytical solution over a 2D regular domain by means of the *Integral Transform Technique* (ITT). In the present work, micro and nano channels with a cross-section geometry typical of chemically etched channels are considered (see Fig. 1). As a consequence, the 2D domain can be either a trapezoid, with an apex angle of θ=54.74°, or a rectangle (θ=90°). The key idea of ITT, originally introduced by Özişik and Murray (1974) and widely used ever since in heat and mass transfer problems (Özişik, 1980; Cotta, 1993), relies on the possibility of writing any function as a linear combination of simple orthonormal functions that represent a basis for the considered domain of definition. In this sense, the transformation is equivalent to a projection of the function along each element of the basis which, for this reason, is also called *kernel* of the transformation. As

shown by Aparecido and Cotta (1990), for both rectangular and trapezoidal geometry it is always possible to perform a transformation, at least in one direction of the 2D cross-sectional domain. Projecting the governing equations along one direction yields a set of M coupled ODEs that depend only on one variable, M being the number of orthogonal bases used to represent all the functions.

Applying the ITT to Eq. (9) is then equivalent to the assumption that the unknown functions can be approximated by means of a finite set of orthonormal functions, namely $\{\psi_j(x,y)\}_{j=1,\cdots,\infty}$, that hinges on the boundary conditions:

$$\begin{cases} \Phi(x,y) \cong \sum_{j=1}^{M} \psi_j(x,y)\overline{\Phi_j}(y) \\ U(x,y) \cong \sum_{j=1}^{M} \psi_j(x,y)\overline{U_j}(y) \end{cases} \quad (11)$$

By means of Eqs. (11) it is possible to perform a transformation of Eq. (7) getting a set of coupled ODEs that can be numerically solved with a specific code written in MATLAB® using the solver for boundary value problems. This code first solves the differential problem and then applies the inverse transform (11) to its solution to compute the unknown functions over the entire cross-section. The solver for the ODEs system is a difference scheme that implements the 3-stage Lobatto IIIA formula, with a relative tolerance of 0.01%, both for the electric potential and the velocity field. Since the required accuracy is not achievable whenever the EDL is very thin even providing the analytical Jacobian of the system, in this work the investigation is limited to electrokinetic diameters smaller than 330. This way, an accuracy of 0.1% could be achieved for almost all the considered cases with a number of terms M of the series defined in Eq.(11) in between 80 and 100.

2.2 Model limitations

The proposed model for electro-osmotic pumping is based on a series of assumptions, most of them implicitly stated. A discussion on their validity is mandatory in order to understand when they no longer hold, especially at the nano scale.

The strongest hypothesis of the model is that of *continuum medium*. This well-known assumption determines the description of the fluid which is further assumed Newtonian. A comprehensive review on the validity of the continuum hypothesis was proposed by Koplik and Banavar (1995), who highlighted that the velocity and stress fields, for both Couette and Poiseuille flows, completely agree with the solution of the Navier-Stokes equations, when no-slip boundary conditions apply, for any channel of width larger than about 10 fluid molecular diameters. The Authors also confirmed the fluid's Newtonian behavior. These conclusions have been recently restated in a review on the nanofluidic transport theory by Sparreboom *et al.* (2010). Strictly related to the validity of continuum equations, it is the validity of their boundary conditions. This is why care has been taken to verify the validity of no-slip boundary conditions for all the cases here analyzed (Cheng and Santiago, 2002; Joly *et al.*, 2006).

Concerning the Poisson equation (Eq. (2)), a flat-wall Boltzmann distribution (Eq. (3)) for all the N ionic-species can be considered valid only if EDLs do not overlap. If they do, ion enrichment and exclusion effects are particularly strong and, as pointed out by Qu and Li (2000) and Baldessari and Santiago (2008), a different EDL model is necessary. However, the same Authors have shown that overlap does not occur if D_e is above 16. For an electrolyte concentration of 10^{-1} M, 10^{-2} M and 10^{-3} M this means that the D_h has to be greater than about, respectively: 17 nm, 50 nm and 150 nm.

In the EOP model previously presented, the Debye-Hückel approximation has been used to linearize the Poisson-Boltzmann equation. This assumption is very often invoked when dealing with electro-osmotic flows, even if its consistency is seldom checked. Since the very first extensive work on the zeta-potential by Hunter (1981), it is known that the fluid composition has a strong influence on the value of the electric potential at the solid/liquid interface, thus a limit on ζ most certainly limits the bulk concentration too. Many experimental data are available in the

literature for both silica and polymeric substrates and a collection of them is reported in the review of Kirby and Hasselbrink (2004). Data show that to have a zeta-potential below *25* mV the bulk concentration must be in between 10^{-1} M and 10^{-2} M, with a pH generally smaller than 6. Only for highly acid solutions concentrations around 10^{-3} M can be considered as well.

This short discussion sets the bounds within which the model can be used properly to characterize open channel EOPs, namely:

1) hydraulic diameters larger than 10 nm so that the continuum assumption holds;
2) molar concentrations of the solution in between 10^{-1} M and 10^{-2} M, so that the Debye-Hückel approximation holds;
3) electrokinetic diameters larger than 16 to avoid the overlap of the EDLs.

3. Numerical characterization

In this section some of the results obtained for open channel EOPs are presented in order to show how the cross-section geometry can influence their performance. As mentioned in section 2.1, chemically etched channels with rectangular and trapezoidal cross-sections are studied varying the aspect ratio ($\beta=h/a$), i.e. the ratio of the height (h) to the smaller base (a) of the channel (Fig. 1).

3.1 Cross-section effects

The behavior of a pump is described by its characteristic curve, which shows the relation between the volumetric flow rate (V) and the pressure head (ΔP). In terms of non-dimensional quantities, the volumetric flow rate can be computed from its definition as:

$$V^* = \iint U(x,y)\,\mathrm{d}x\,\mathrm{d}y \qquad (12)$$

while the pressure head is equivalent to the non-dimensional number G_{EO} for a fixed bulk composition and a given applied electric field. Some non-dimensional characteristic curves for a rectangular channel (no markers) and a trapezoidal channel (triangular markers) for two different values of the aspect ratio are shown in Fig. 2a, where the non-dimensional zeta-potential is equal to 1 and D_e=164.41. The figure shows that curves greatly hinge on the geometry of the cross-section. Comparing the behavior for the same θ, it is evident that a reduction of the aspect ratio leads to a better performance both in terms of volumetric flow rate and of G_{EO}. On the other hand, rectangular and trapezoidal cross-sections at the same aspect ratio show a significant difference in the behavior only for low values of G_{EO}. To better understand the dependence of V^* on G_{EO}, in Fig. 2b the trend of the dimensionless velocity field along the centerline of the cross-section of the square channel (θ=90º, β=1) is shown for points A, B and C of Figure 2a.

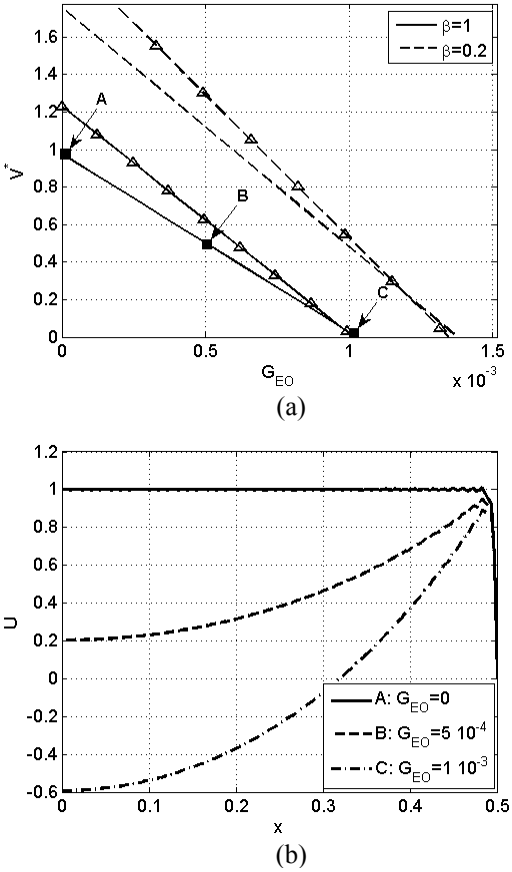

Fig. 2. Characterization of a single open channel EOP for θ=90° (■) and θ=54.74° (Δ) at Z=1 and D_e=164.41: (a) characteristic curves; (b) velocity profiles.

The effect of the imposed back pressure is evident: when G_{EO} increases, the velocity profile is no longer flat, but an inflection starts from the core of the channel decreasing the net flow rate. The value of G_{EO} for which the net flow rate vanishes (point C in Fig. 2a) has been called *critical* G_{EO} ($G_{EO,c}$). An operating condition corresponding to the point C in Fig.

2a should be avoided and is presented here as a limiting case. Fig. 2b suggests to limit the operative values of G_{EO} from 0 to about 0.5 times the critical value, thus the point B of Fig. 2a can still be a possible working point, while the stretch between B and C represents conditions to be avoided because of a flow reversal. Moreover, whenever a choice is possible, it is better to work at the highest value of G_{EO} that can be achieved without the occurrence of a backflow, mainly because of two reasons. First of all, for a given bulk composition and an imposed electric field, a large operative G_{EO} corresponds to a large pressure head. Conversely, fixing the pressure head and the fluid, a high G_{EO} is equivalent to a low applied electric voltage, and therefore to a small power consumption. This improves the efficiency of the EOP.

Characteristic curves of EOPs are linear, so they are completely defined by two operating conditions. In particular it is of interest to consider those representing the two limiting conditions, i.e. the maximum flow rate (point A) and the maximum pressure head (point C). Analyzing these specific quantities is equivalent to studying and comparing the whole characteristic curves.

In Fig. 3 trends of the maximum non-dimensional volumetric flow rate (V^*_{max}), which corresponds to G_{EO}=0, as a function of D_e are plotted for a single open channel EOP with a trapezoidal cross-section and Z=1 for several βs. The trends show that higher values of D_e and lower values of β provide larger volumetric flow rates for any value of the zeta-potential. However, while V^*_{max} increases by 20% if D_e increases by one order of magnitude, it becomes about three times greater if β decreases from 0.5 to 0.1. Fig. 3 also shows that the same maximum volumetric flow rate is achievable with different combinations of the aspect ratio and of the electrokinetic diameter. This means that if some kind of constraint bounds one of the two parameter, the other one can be chosen in order to get the desired flow rate.

In Fig. 4 trends of the critical G_{EO} ($G_{EO,c}$), which corresponds to V^*=0, as a function of β are plotted for three values of D_e for the case described in Fig. 3. Higher values of the critical G_{EO} can be attained reducing the value both of D_e and of β. These results show that the ability to handle a back pressure inside any channel is enhanced by a more homogeneous distribution of the electric forces over the cross-section. Pressure body forces are uniformly distributed on each section, while electrical body forces exist only in the EDL, where charges are: whenever the EDLs occupy a significant portion of the channel, electrical body forces can handle the back pressure more easily and this happens when D_e or β decrease.

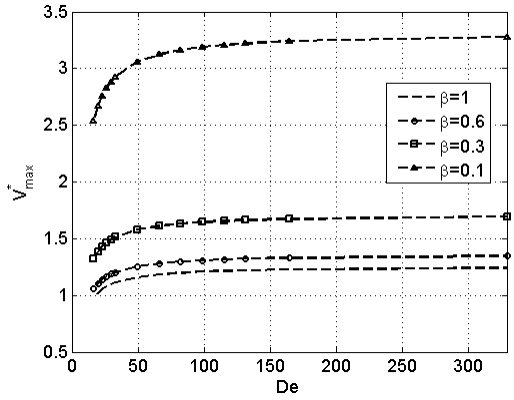

Fig. 3. Maximum volumetric flow rate (G_{EO}=0) of a single open channel EOP for θ=54.74° and Z=1 as functions of the electrokinetic diameter and of the aspect ratio.

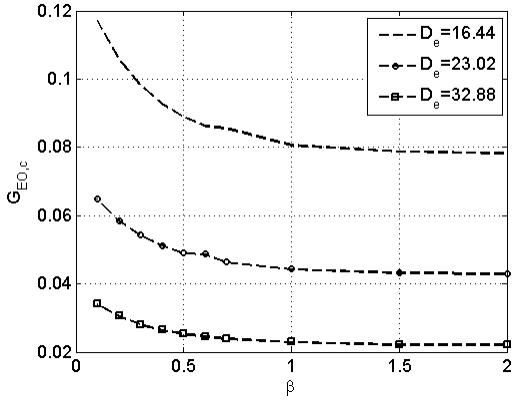

Fig. 4. Critical G_{EO} (V^*=0) of a single open channel EOP for θ=54.74° and Z=1 as a function of the electrokinetic diameter and of the aspect ratio.

Figs. 3 and 4 show also that, while the aspect ratio has the greatest influence on the flow rate, the electrokinetic diameter affects the critical G_{EO} the most, especially if D_e is between 16 and 50. An increase by almost one

order of magnitude can occur scaling down D_e within this range, while a variation of about 30% is achieved if β varies from 0.5 to 0.1.

Similar conclusions hold both for the maximum flow rate and for $G_{EO,c}$ also if the channel has a rectangular cross-section.

3.2 Correlations for EOPs performance

Results presented so far can help in the design of open channel EOPs with single or multiple micro channels. However, to study the behavior of a particular EOP a specific code, like the one implemented for the present work, should be employed. A way to make the model and its results easily available is the determination of simple correlations for the prediction of the pump performance, that is, the determination of simple expressions for the maximum flow rate and for the critical G_{EO}. If these quantities are known, designers can easily draw the characteristic curve of any open channel silicon EOP.

The main parameters affecting the EOP behavior are the following:

1) the dimensionless zeta-potential Z,
2) the apex angle θ of the cross section,
3) the aspect ratio β of the cross section,
4) the electrokinetic diameter D_e.

Concerning the dependence of the volumetric flow rate and of the pump pressure head on the dimensionless zeta-potential, comparing all the simulations it is possible to conclude that the maximum non-dimensional flow rate is completely unaffected by Z, while the critical G_{EO} is directly proportional to it. This is due to the linearization introduced with the Debye-Hückel approximation and means that:

$$\begin{cases} V^*_{\max}(\theta,\beta,D_e,\mathrm{Z}) = V^*_{\max}(\theta,\beta,D_e,1) \\ G_{EO,c}(\theta,\beta,D_e,\mathrm{Z}) = G_{EO,c}(\theta,\beta,D_e,1) * \mathrm{Z} \end{cases} \quad (13)$$

at least until this assumption holds. In Eq. (13) the dependence of both the reference quantities on the other three parameters (θ, β, D_e) is not explicit. To obtain this dependence an interesting approach is related to the application of the known analytical expressions for parallel plates to finite cross-section channels.

Considering the work of Chen and Santiago (2002) and the non-dimensional quantities introduced in section 2.1, it follows that the maximum flow rate for a rectangular channel can be written as:

$$V^{*pp}_{\max} = A \cdot f(D_e/2) = A \cdot \left(1 - \frac{\tanh(D_e/2)}{D_e/2}\right) \quad (14)$$

where A is the area of the cross-section, while for the critical G_{EO}, at Z=1, the expression is:

$$G^{pp}_{EO,c} = \frac{12}{D_e^2} \cdot f(D_e/2) \quad (15)$$

A comprehensive analysis of the results shows that the reference quantities in Eq. (13) can be determined referring to Eqs. (14) and (15) as follows (Geri *et al.*, 2011):

$$\begin{cases} V^*_{\max} = V^{*pp}_{\max} \cdot f(D_e/2) \\ G_{EO,c} = 2 \cdot G^{pp}_{EO,c} f(D_e/2) g(\beta) \end{cases} \quad (16)$$

where the function $g(\beta)$ has a double exponential dependence on the aspect ratio:

$$g(\beta) = a \cdot \exp(b \cdot \beta) + c \cdot \exp(d \cdot \beta) \quad (17)$$

and its coefficients (a, b, c, d), that can be obtained fitting the numerical results presented in section 3.1, are listed in Table 1.

Table 1
Fitting coefficients for the function $g(\beta)$.

a	*b*	*c*	*D*
0.815452	-3.75009	1.18041	$2.06422 \cdot 10^{-2}$

Equations (16) and (17) hold for Z=1, for both rectangular and trapezoidal cross-sections with an electrokinetic diameter between 16 and 330 and an aspect ratio down to 0.001. The upper limit for the aspect ratio is 1 and 2 for rectangular (θ=90°) and trapezoidal cross-sections (θ=54.74°) respectively. It is worth noting that Eq. (16) is the result of theoretical considerations regarding the effect of the channel walls on the pump behavior. In particular, the effect of the electrokinetic diameter can be taken into account considering each pair of opposite walls of the finite cross-section as two parallel plates. Only the dependence on the aspect ratio for the critical G_{EO} needs to be introduced and numerically computed, since a simple correlation with the area of the cross-section is not possible. Using Eqs. (13)-(17) with the coefficients of Table 1 all the characteristic curves for pumps with the

aforementioned geometrical and electrical features can be obtained. The relative error between numerical results and the results obtained by this correlation in the specified ranges is always smaller than 2%.

4. Conclusions

In this work a numerical investigation of the behavior of silicon DC open channel electro-osmotic pumps has been performed to evidence the influence of the cross-sectional geometry and of the fluid electrical properties on the pump behavior. Micro and nano channels with trapezoidal (θ=54.74°) and rectangular (θ=90°) cross-sections have been analyzed for several values of the aspect ratio and of the electrokinetic diameter.

Dimensionless characteristic curves (volumetric flow rate vs. head pressure) have been obtained to evaluate the performance of the pump. It has been shown that the aspect ratio strongly influences the maximum flow rate, while the electrokinetic diameter mostly affects the maximum pressure head. Decreasing β increases both the non-dimensional volumetric flow rate and the pump pressure head, while an increase of D_e increases the flow rate but at the same time decreases the pressure head.

With the aim of giving a useful tool to the EOPs designers, two correlations have been developed for both rectangular and trapezoidal geometries. These correlations take into account all the parameters that affect the pump behavior and allow to draw the characteristic curve of any silicon open channel EOP within the constraints of the presented model.

References

Aparecido, J.B., Cotta, R.M., 1990. Laminar flow inside hexagonal ducts. Comp. Mech. 6, 93 – 100.

Arulanandam, S., Li, D., 2000. Liquid transport in rectangular microchannels by electroosmotic pumping. Colloid Surface A 161, 89 – 102.

Baldessari, F., Santiago, J.G., 2008. Electrokinetics in nanochannels.Part I:EDL overlap and channel-to-well equilibrium. J. Col. Int. Sci. 325, 526 – 538.

Bruus, H. 2007. Theoretical microfluidics. Oxford University Press.

Burgreen, D., Nakache, F.R., 1964. Electrokinetic flow in ultrafine capillary slits. J. Phys. Chem. 68, 1084 – 1091.

Chen, C.H., Santiago, J.G., 2002. A planar electroosmotic micropump. J. Microelectromech. S. 11, 672 – 683.

Cheng J.T., Giordano, N., 2002. Fluid flow through nanometer-scale channels. Phys. Rev. E 65, 031206.

Conlisk, A.T., 2005. The Debye-Hückel approximation: its use in describing electroosmotic flow in micro- and nanochannels. Electrophoresis 26, 1896 – 1912.

Cotta, R.M., 1993. Integral Transform in computational heat and fluid flow. CRC Press.

Geri, M., Lorenzini, M., Morini, G.L., 2011. Wall effect on the performance of DC electro-osmotic micro and nano pumps. Proceedings of the UIT Conference, Torino, Italy.

Hildreth, D., 1970. Electrokinetic flow in fine capillary channels. J. Phys. Chem. 74, 2006 – 2015.

Hunter, R.J., 1981. Zeta Potential in Colloidal Science: Principle and Applications. London Academic Press.

Joly, E.T.L., Ybert, C., Bocquet, L., 2006. Liquid friction on charged surfaces: from hydrodynamic slippage to electrokinetics. J. Chem. Phys. 125.

Karniadakis, G., Beskok, A., Aluru, N., 2005. Microflows and Nanoflows: Fundamentals and Simulation. Springer, NY.

Kirby, B.J., Hasselbrink Jr, E.F., 2004. Zeta potential of microfluidic substrates. Electrophoresis 25, 187 – 202.

Koplik, J., Banavar, J., 1995. Continuum deductions from molecular hydrodynamics. Ann. Rev. Fl. Mech. 27, 257-292.

Laser, D.J., Santiago, J.G., 2004. A review of micropumps. J. Micromech. Microeng. 14, R35 – R64.

Lazar, I.M., Karger, B.L., 2002. Multiple open-channel electroosmotic pumping system for microfluidic sample handling. Anal. Chem. 74, 6259 – 6258.

Litster, S., Suss, M.E., Santiago, J.G., 2010. A two-liquid electroosmotic pump using low applied voltage and power. Sensor Actuator A. 163, 311 – 314.

Manz, A., Graber, N., Widmer, H.M., 1990. Miniaturized total chemical analysis system: a novel concept for chemical sensing. Sensor Actuator B. 1, 244 – 248.

Masliyah, J.H., Bhattacharjee, S., 2006. Electrokinetic and colloid transport phenomena. John Wiley&Sons.

Morini, G.L., 2004. Single-phase convective heat transfer in microchannels: a review of experimental results. Int. J. Therm. Science, 43, 631 – 651.

Özişik, M.N., 1980. Heat Conduction. 2nd Edition, New York Wiley.

Özişik, M.N., Murray, R.L., 1974. On the solution of linear diffusion problems with variable boundary condition parameters. ASME paper 74-HT-1.

Probstein, R.F., 1994. Physicochemical Hydrodynamics. 2nd ed. New York Wiley.

Qu, W., Li, D., 2000. A model for overlapped EDL fields. J. Colloid Interf. Sci. 224, 397 – 407.

Sparreboom, W., van den Berg, A., Eijkel, J.C.T., 2010. Transport in nanofluidic system: a review of theory and applications. New J. Phys. 12, 015004.

Rice, C.L., Whitehead, R., 1965. Electrokinetic flow in a narrow cylindrical capillary. J. Phys. Chem. 69, 4017 – 4024.

Wang, X., Wang, S., Gendhar, B., Cheng, C., Byun, C.K., Li, G., Zhao, M., Liu, S., 2009. Electroosmotic pumps for microflow analysis. Trends Analyt. Chem. 28, 64 – 74.

Yao, S., Santiago, J.G., 2003. Porous Glass electroosmotic pumps: theory. J. Coll. Int. Science, 268, 133 – 142.

Yao, S., Hertzog, D.E., Zeng, S., Mikkelsen Jr., J.C., Santiago, J.G., 2003. Porous Glass electroosmotic pumps: design and experiments. J. Coll. Int. Science, 268, 143 – 153.